Notch activity acts as a sensor for extracellular calcium during vertebrate left–right determination

Ángel Raya[1]*, Yasuhiko Kawakami[1]*, Concepción Rodríguez-Esteban[1]*, Marta Ibañes[1], Diego Rasskin-Gutman[1], Joaquín Rodríguez-León[2], Dirk Büscher[1], José A. Feijó[2,3] & Juan Carlos Izpisúa Belmonte[1]

[1]*Gene Expression Laboratory, The Salk Institute for Biological Studies, 10010 North Torrey Pines Road, La Jolla, California 92037, USA*
[2]*Instituto Gulbenkian de Ciencia, Rua Da Quinta Grande n6, 2780-901 Oeiras, Portugal*
[3]*Centro de Biotecnologia Vegetal, Faculdade de Ciencias, Universidade Lisboa, 1749-016 Lisboa, Portugal*

* These authors contributed equally to this work

During vertebrate embryo development, the breaking of the initial bilateral symmetry is translated into asymmetric gene expression around the node and/or in the lateral plate mesoderm. The earliest conserved feature of this asymmetric gene expression cascade is the left-sided expression of *Nodal*, which depends on the activity of the Notch signalling pathway. Here we present a mathematical model describing the dynamics of the Notch signalling pathway during chick embryo gastrulation, which reveals a complex and highly robust genetic network that locally activates Notch on the left side of Hensen's node. We identify the source of the asymmetric activation of Notch as a transient accumulation of extracellular calcium, which in turn depends on left–right differences in H^+/K^+-ATPase activity. Our results uncover a mechanism by which the Notch signalling pathway translates asymmetry in epigenetic factors into asymmetric gene expression around the node.

The disposition of most internal organs in vertebrates shows evident asymmetries along the left–right (LR) axis. The acquisition of proper LR asymmetries is achieved in a highly consistent manner during early embryo development. An evolutionarily conserved feature in the process of LR determination is the biased expression of *Nodal* in the left lateral plate mesoderm (LPM; reviewed in refs 1–5). Transgenic studies in mice have shown that left-sided expression of *Nodal* in the LPM depends on an earlier domain of *Nodal* expression around the node[6,7].

Notch activity plays an important role in the early phases of LR determination by directly regulating *Nodal* expression around the node in mouse[8,9] and zebrafish[9] embryos. The activity of the Notch signalling pathway depends on the complex interplay of several receptors, ligands and modulators (reviewed in ref. 10). In an effort to identify factors that regulate Notch activity around the node, we have characterized the dynamics of gene expression and interactions among relevant genes and proteins of this signalling pathway during early embryo gastrulation, and have generated a mathematical model to help us pinpoint those factors that are essential in LR determination.

LR asymmetry in components of the Notch pathway

We chose the chick embryo as the experimental model for these studies because of its unrivalled amenability for gene expression analysis during gastrulation, and also because *Nodal* expression around Hensen's node in the chick is overtly asymmetric during a sizeable window of time. We first investigated whether Notch activity is necessary for establishing proper LR asymmetry during chick embryo development. Indeed, blocking the Notch signalling pathway by overexpressing a dominant-negative form of the Notch pathway effector Suppressor of Hairless (Su(H)) resulted in laterality defects at both the morphological and the molecular level (see Supplementary Fig. 1), similar to those described for mouse embryos[8,9].

We then analysed the expression patterns of the known Notch genes (*Notch1–Notch3*) and ligands (*Delta-like 1* (*Dll1*), *Delta-like 3*, *Delta-like 4*, *Serrate1* and *Serrate2*), as well as those of the Notch pathway modulators *Lunatic fringe* (*Lfng*) and *Radical fringe*, in chick embryos from Hamburger and Hamilton stage 3 (HH3) to HH8 (ref. 11) by *in situ* hybridization, and compared them with that of *Nodal*. The transcripts with a potential role in establishing LR asymmetry on the basis of their expression pattern are summarized in Fig. 1 (see also Supplementary Fig. 2). From these analyses it became evident that, before the appearance of the left-sided peri-nodal expression domain of *Nodal*, the Notch ligands *Dll1* and *Serrate1* show complementary patterns of expression that form a sharp anterior–posterior (AP) interface across Hensen's node (Fig. 1b, g, h).

Notably, *Dll1* transcripts at HH5 extended more anteriorly on the left side of the node in most embryos analysed (85%, $n = 125$; Fig. 1b, g). This asymmetry in *Dll1* expression is the earliest indication that Notch activity may be differentially lateralized. During HH3–HH7, *Lfng* is expressed in a complex, dynamic pattern of waves that sweep the AP axis of the embryo[12]. We noticed that the fifth wave of *Lfng* is clearly asymmetric when it reaches the node at HH6: the medial-most part of the left stripe is anteriorly displaced with respect to the right (Fig. 1d). The location of the left-sided expression domain of *Nodal* at HH6 seems to coincide with the asymmetric region of *Dll1* expression previously established at HH5 (Fig. 1, compare e with b) and also overlaps with the anterior displacement of *Lfng* expression (Fig. 1, compare e with d).

Mathematical modelling of Notch activation

To gain a better understanding of the molecular mechanisms governing LR asymmetry determination and to be able to predict specific schemes that could be tested experimentally, the qualitative data collected from our gene expression analyses were used to model mathematically the dynamics of Notch activation during this process. The target of our model was to express *Nodal* differentially on the left side of the node while maintaining the hypothesis that the same mechanisms of signalling and interaction between cells operate in both the left and right peri-nodal regions.

We devised a network of interactions among messenger RNAs and proteins representing Notch1, Dll1, Serrate1 and Nodal (Fig. 2a). In brief, on the basis of the asymmetries detected in our gene expression analyses (Fig. 1) and the fact that Fringe has key roles in modulating Notch activity in several developmental contexts[13–16], we introduced *Lfng* as an external network modulator (see Fig. 2, Box 1 and Supplementary Methods). Furthermore, taking into account that LR asymmetries have been described to occur at stages earlier than HH4 (refs 1–4), we introduced a second external modulator acting along the LR axis in our model (see below).

Two assumptions in our theoretical model are that *Dll1* expression is induced by Notch activity, and that juxtaposition of *Dll1* and *Serrate1* expression domains strengthens Notch activity (Fig. 2a). To test the first assumption experimentally, we downregulated Notch signalling either by using DAPT (*N*-[*N*-(3,5-difluorophenacetyl-L-alanyl)]-*S*-phenylglycine *t*-butyl ester), a γ-secretase inhibitor known to block the Notch pathway *in vivo*[17], or by overexpressing a dominant-negative version of Su(H). Either treatment resulted in a marked downregulation of *Dll1* expression (39% and 35%, $n = 80$ and $n = 95$, respectively; Fig. 3a–d).

To challenge experimentally the theoretical assumption that complementarities of *Dll1* and *Serrate1* expression domains are needed for proper Notch activity around Hensen's node, we removed Dll1 function by ectopically expressing a dominant-negative form of *Dll1* in the peri-nodal region. Embryos cultured in these conditions failed to activate left-sided expression of *Nodal* (38%, $n = 60$; Fig. 3e, f) and showed reversed heart looping (28%, $n = 48$; Fig. 3g). We also addressed the role of the juxtaposition of *Dll1* and *Serrate1* expression domains more directly by ubiquitously expressing *Dll1* in HH3–HH4 chick embryos. Notably, this manipulation resulted in alterations in LR patterning similar to those elicited by dominant-negative *Dll1* (87%, $n = 25$; Fig. 3h).

The positive role of *Lfng* as a modulator of Notch activity during LR determination was also tested experimentally. Our mathematical model considers that *Lfng* indirectly induces left-sided asymmetrical expression of *Dll1* at HH5 and directly activates the Notch pathway such that *Nodal* becomes expressed. This was experimentally confirmed by the retroviral delivery of *Lfng*, which caused ectopic right-sided expression of *Nodal* (48%, $n = 73$; Fig. 3i, j) and alterations in heart looping (34%, $n = 40$; Fig. 3k, l). Overall, our theoretical and experimental results underscore the importance of the juxtaposition of gene expression domains in biological design. Specifically, and during the establishment of LR asymmetries, the hyperactivation of Notch occurs precisely at the juxtaposition of *Dll1* and *Serrate1* expression and is strengthened where *Lfng* is expressed.

To identify potential modulators of Notch activity on the left or right side of Hensen's node, we mathematically explored the response generated by our model under different parameter values for specific initial conditions. Notably, our simulations show that *Dll1* and *Nodal* can be expressed asymmetrically by varying the binding rates of the complexes Notch1–Dll1 and Notch1–Serrate1. Thus, we find that the action of the LR modulator on binding rates is the most parsimonious way to reproduce the left and right expression patterns during stages HH4–HH6 (Fig. 2b, c).

In our model, *Lfng* provides a mechanism that ensures the appearance of *Nodal* by highly activating the Notch pathway. In a sense, this mechanism would operate as a synchronizer that would allow *Nodal* expression to be switched on at a very specific location and time (when the fifth *Lfng* wave sweeps the *Dll1-Serrate1* interface), rather than as an essential component of the system (Fig. 3m). This theoretical conclusion is in agreement with the absence of LR defects in mice that are mutant for *Lfng* (refs 14, 15; T. Gridley and R. Johnson, personal communications) and hints at the robustness of the system (understanding 'robustness' as constancy of outcome despite perturbations[18]).

In fact, one of the more noticeable properties of the genetic network characterized in our model is that it translates small variations in binding rates for the Notch–Dll1 and Notch–Serrate1 complexes into robust, side-specific expression of *Nodal*. The

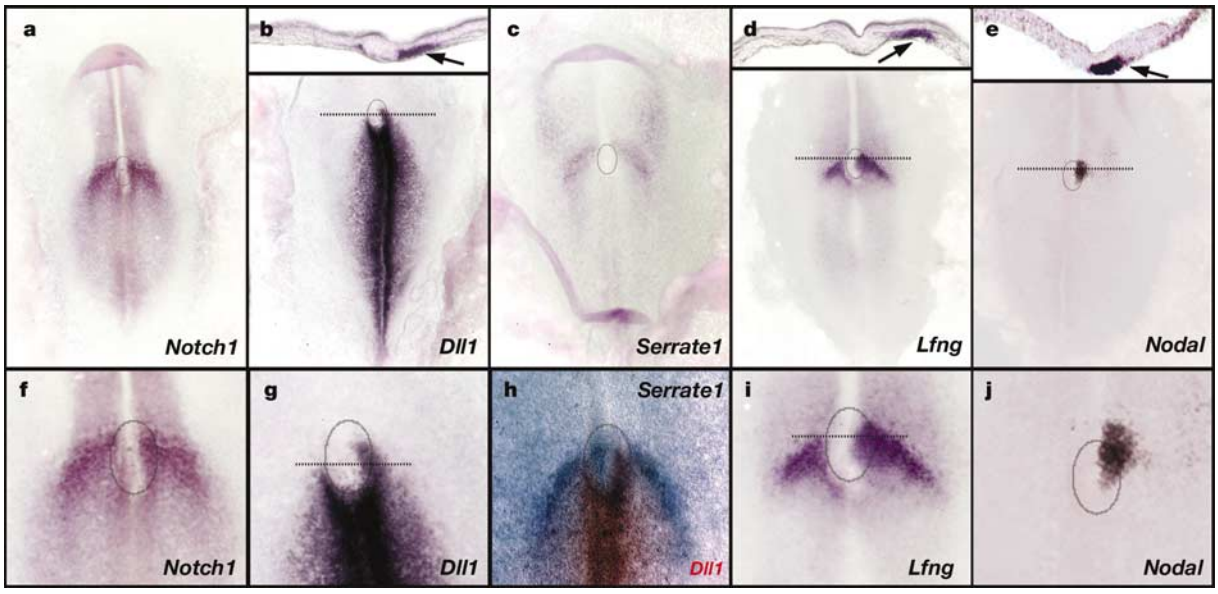

Figure 1 Asymmetries in the expression of Notch pathway components during chick gastrulation. **a**, *In situ* hybridization of HH6 chick embryos shows symmetrical expression of *Notch1* transcripts above Hensen's node. **b**, At HH5, *Dll1* transcripts become asymmetric in Hensen's node (dotted line in main panel). *Dll1*-positive cells are present on the left side of Hensen's node but are absent on the right side. In addition, *Dll1* transcripts extend anterior to the left side of Hensen's node (arrow in section shown on top). **c**, *Serrate1* transcripts at HH6 are observed in the form of two symmetrical stripes above and lateral to Hensen's node. **d**, At HH6, *Lfng* expression becomes asymmetric around Hensen's node: the left stripe extends more medially and anteriorly than the right one (dotted line in main panel, arrow in section on top). **e**, *Nodal* transcripts appear at HH6, showing a clear signal on the left anterior side of Hensen's node (dotted line in main panel, arrow in section shown on top). **f**, **g**, **i**, **j**, Higher magnification of **a**, **b**, **d**, **e**, respectively, showing symmetric expression of *Notch1* and left-sided asymmetric expression of *Dll1*, *Lfng* and *Nodal*. **h**, Double-colour *in situ* hybridization for *Dll1* (red) and *Serrate1* (blue) in HH5 chick embryos, illustrating the juxtaposition of expression domains. All panels are ventral views, anterior is to the top. Ovals mark the position of Hensen's node.

system's ability to buffer perturbations is also reflected in our model, which tolerates not only the malfunction of *Lfng* (Fig. 3m) but also large fluctuations in several parameters (a detailed exploration of the sensitivity of the parameters is provided in Supplementary Methods), while allowing the normal left-sided expression of *Nodal*.

Notch activation depends on H^+/K^+-ATPase activity

Our mathematical model predicts that a local domain of Notch hyperactivation reflects a pre-existing, transient LR asymmetry. Several factors and mechanisms are involved in the early events that break the initial bilateral symmetry in the embryo[19–21]. Among them, the nodal flow created by monociliated cells in the mouse node[22,23] seems to function in a parallel mechanism of LR determination that is unrelated to the one used by Notch[8,9]. In addition, Sonic hedgehog (Shh), a signalling molecule that mediates left-

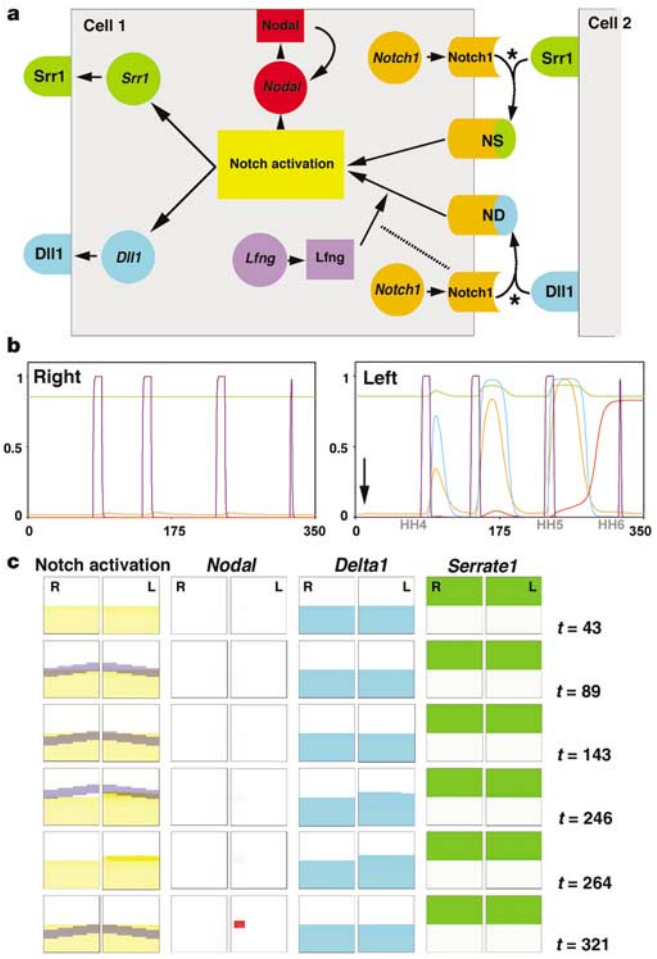

Figure 2 Mathematical model characterizing Notch activation dynamics. **a**, Network model. Circles symbolize mRNA, boxes represent proteins or protein complexes (ND, Notch1–Dll1; NS, Notch1–Serrate1). Two cells are shown. In cell 1, the full set of interactions can be seen. Asterisks denote the action of the external LR modulator in the formation of Notch complexes. The broken line indicates the regulation of Lfng action by Notch (see Box 1). **b**, Variation over time of Notch activation and *Nodal*, *Dll1* and *Serrate1* expression measured just above the *Dll1–Serrate1* interface (colour coding as in a). Arrow indicates the introduction of the external LR modulator. **c**, Simulation snapshots of gene expression and Notch activity. We consider the two lattices (left and right peri-nodal regions) to be initially equivalent. At time $t = 9$ min, the LR modulator is introduced on the left side. Later, four waves of *Lfng* sweep the left and right lattices, leading to transient asymmetric expression of *Dll1* more anteriorly and expression of *Nodal* only in the left peri-nodal region.

Box 1

A dynamic model of peri-nodal Notch activation

The mathematical model accounts for the formation of two complexes, Notch1–Dll1 (ND) and Notch1–Serrate1 (NS), which regulate a signalling pathway downstream of Notch1, called Notch activation (NA). We simplified this signal cascade into two steps: first, the receptor–ligand complexes activate the cascade; second, this cascade activates the mRNAs of *Dll1*, *Serrate1* and *Nodal* (refs 8, 9, 43, and Fig. 3). In addition, Nodal activates its own production via a positive feedback loop. The posterior regression of the node is also taken into account so that at stage HH4 the *Dll1–Serrate1* interface is just posterior to the node, whereas at stage HH6 it is anterior. *Lfng* appears dynamically as a wave that sweeps both lattices four times in a postero-anteriorly direction up to the most anterior part of the node, thereby influencing the activation of the Notch pathway cell autonomously[12,44]. *Lfng* is known to encode a glycosyltransferase that acts on Notch protein[45,46]. Several roles have been proposed for Fringe-mediated Notch signalling pathway modulation. We assume that Lfng modifies Notch so that its activity is enhanced on forming the complex with Delta.

A pair of independent two-dimensional lattices (left and right) of 16×32 cells is taken to characterize the peri-nodal left and right regions, respectively. In each lattice, every single cell is characterized by the amount of mRNA, protein and protein complexes, as well as by their mutual interaction (see Fig. 2a). The model has been formulated as a set of 13 coupled nonlinear delay and ordinary differential equations for each cell (see Supplementary Methods). The dynamics of each molecular species is a balance of its production (mRNA transcription and protein translation), its decay rate and the binding rate of complex formation. The interaction among macromolecular species is described according to mass-action kinetics. The pseudo steady-state approximation for activation rates is also taken into account.

Thus, if we consider that the dynamics of y are controlled by the activation through x and its own decay, the dynamic equations for y read:

$$\frac{dy}{dt} = \psi_\kappa(x,h) - y; \psi_\kappa(x,h) = \frac{x^\kappa}{x^\kappa + h^\kappa}$$

where ψ_κ is a saturating function with stiffness controlled by the Hill or cooperative coefficient (κ, ref. 47), and parameter h is a measure of the threshold value above which activation is greater than 50%. By way of example, the equations for *Dll1* (*Dll*), Dll1 (Dll) and NA are written below:

$$\frac{d\mathrm{Dll}_i(t)}{dt} = a_d\psi_3(\mathrm{NA}_i(t), h_d) - \mu_d \mathrm{Dll}_i(t) \quad (1)$$

$$\frac{d\mathrm{Dll}_i(t)}{dt} = t_D \mathrm{Dll}_i(t - T_D) - b_{\mathrm{ND}} \sum_{j \in nn(i)} \mathrm{Dll}_i(t)\mathrm{Notch}_j(t) - \mu_D \mathrm{Dll}_i(t) \quad (2)$$

$$\frac{d\mathrm{NA}_i(t)}{dt} = a_{\mathrm{NA}}\psi_2(A[\mathrm{Lfng}_i(t)/\mathrm{Notch}_i(t)] \cdot \mathrm{ND}_i(t) + B \cdot \mathrm{NS}_i(t), h_{\mathrm{NA}}) - \mu_{\mathrm{NA}}\mathrm{NA}_i(t) \quad (3)$$

Equation (1) indicates that the activation of *Dll* in cell i depends on NA. If the Notch pathway is not active (NA = 0), then *Dll* is not expressed. As NA increases, *Dll* expression is enhanced until it saturates at a maximum stationary value of $\mathrm{Dll}_{\max} = \frac{a_d}{\mu_d}$, where a_d and μ_d are the transcription and decay rates respectively. As shown by the last term of equation (1), first order decay processes have been considered. According to equation (2), the change rate of Dll1 concentration depends on *Dll1* translation, Dll1 binding to Notch receptors in neighbouring cells and its decay rate. The delay term accounts for the time needed by large proteins to be translated, to be transported to the membrane and to become active (T_D). The communication between cells is established through juxtacrine (nearest neighbours, *nn(i)*) ligand–receptor interactions[48–50]. In addition, equation (3) accounts for the activation of the Notch pathway through ND and/or NS. The ability of each complex to activate the Notch pathway is different; it is greater for ND, which is also modulated by Lfng.

sided expression of *Nodal* in the LPM[20], does not influence peri-nodal Notch activity[9]. It has been proposed that LR differences in H^+/K^+-ATPase activity occur early during LR determination in chick embryos, resulting in gradients in membrane potential, and that this differential activity is crucial for proper LR establishment[24]. These findings, however, do not explain how the initial symmetry is broken in the first place[25], or how the differential H^+/K^+-ATPase activity is translated into asymmetric gene expression around the node[26].

To investigate whether the Notch signalling pathway has a role in translating this differential activity, we analysed the appearance of the activation domain of Notch after inhibiting the H^+/K^+-ATPase with omeprazole. Treatment of chick embryos with this compound results in bilateral expression of *Nodal* in the LPM (30%, $n = 18$; Fig. 4a, b; see also ref. 24). Notably, this treatment also induces a loss of asymmetric expression of *Dll1* (68%, $n = 52$; Fig. 4c, d) and *Lfng* (72%, $n = 40$; Fig. 4e, f) around Hensen's node. In addition, the expression of *Nodal* in the left peri-nodal region is greatly reduced after treatment with omeprazole (65%, $n = 30$; Fig. 4g, h). Despite this local decrease in *Nodal* transcripts, we could detect *Nodal* expression in the LPM, which at times was bilateral. We identified the origin of this ectopic *Nodal* expression in the fact that omeprazole treatment induces ectopic *Shh* expression (ref. 24 and Supplementary Fig. 3). These results indicate that the activity of the H^+/K^+-ATPase may be at the base of the asymmetric event responsible for the appearance of Notch activation on the left side of Hensen's node.

LR asymmetry in extracellular Ca^{2+}

A differential H^+/K^+-ATPase activity across Hensen's node creates a gradient in membrane potentials, which in turn is likely to originate a differential ion flux across the LR axis[24]. It has been proposed that molecules that are small enough to pass through gap junctions and that are charged under physiological conditions will be accumulated on one side of the embryo's node; the proposed candidates include Ca^{2+}, inositol phosphates, cyclic nucleotides and neurotransmit-

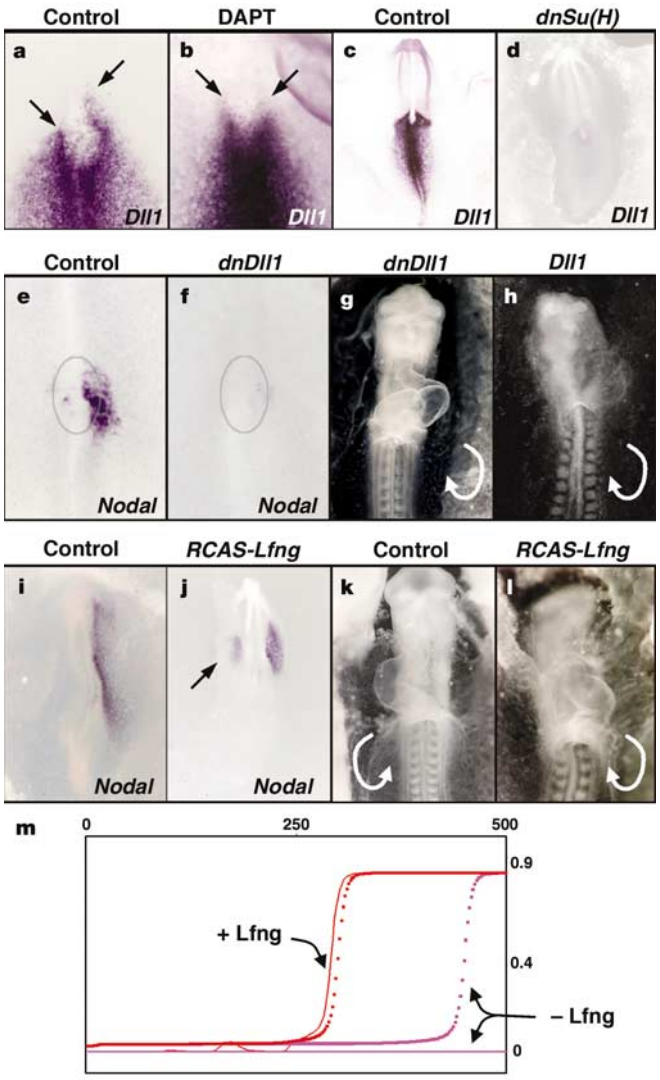

Figure 3 Experimental test of the theoretical assumptions and predictions. **a**, **b**, Downregulation of Notch signalling by treatment with the γ-secretase inhibitor DAPT resulted in loss of the left asymmetric domain of *Dll1* expression (**b**, compare with control in **a**). Arrows point to anterior expression around Hensen's node. **c**, **d**, Overexpression of a dominant-negative form of the Notch effector Su(H) [*dnSu(H)*] downregulated *Dll1* expression in HH8 embryos (**d**, compare with control in **c**). **e**–**h**, Disruption of the *Dll1–Serrate1* expression interface by overexpressing a dominant-negative form of *Dll1* (*dnDll1*) resulted in a failure to activate left-sided *Nodal* expression (**f**, compare with control in **e**) and reversed heart looping (**g**). Similar phenotypic alterations in LR patterning were obtained after ubiquitous expression of *Dll1* (**h**). **i**–**l**, Compared with control embryos (**i**, **k**), ectopic expression of *Lfng* activated ectopic *Nodal* expression in the right LPM (arrow in **j**) and resulted in alterations of the normal rightward looping of the heart tube (**l**). All embryo images are ventral views, anterior is to the top. Ovals mark the position of Hensen's node. Semicircular arrows indicate direction of heart looping. **m**, Numerical results of our theoretical model for the temporal evolution of *Nodal* expression in the left peri-nodal region in normal conditions (red lines) and in conditions simulating *Lfng* ablation (pink lines). Unbroken lines are registered in a cell in the juxtaposed expression domain; broken lines correspond to cells in the *Dll1* domain exactly at the border with *Serrate1*. Lfng action results in a broader and earlier domain of *Nodal* expression.

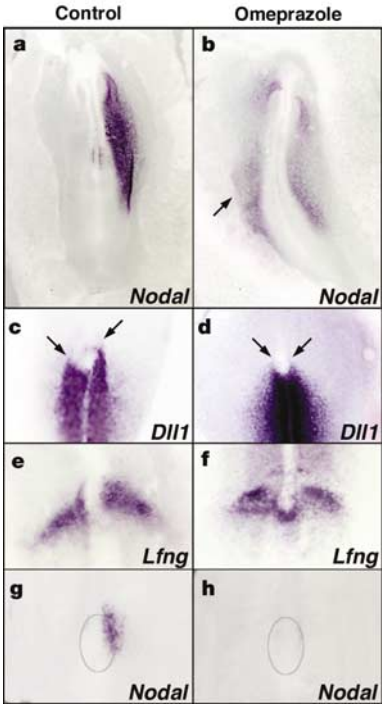

Figure 4 Differential H^+/K^+-ATPase activity regulates Notch signalling during LR determination. **a**, **b**, Treatment of HH3–HH4 chick embryos with omeprazole, a pharmacological inhibitor of H^+/K^+-ATPase, caused ectopic expression in the right LPM of *Nodal* (**b**, arrow). **c**–**f**, Treatment of chick embryos with omeprazole also prevented the appearance of the left-sided asymmetric expression domain of *Dll1* (**c**, **d**) and *Lfng* (**e**, **f**). Arrows point to anterior expression around Hensen's node. **g**, **h**, Analysis of *Nodal* expression after omeprazole treatment shows a downregulation of *Nodal* transcripts in the peri-nodal region (**h**). All panels are ventral views, anterior is to the top. Ovals mark the position of Hensen's node.

ters[27]. Because our theoretical model underscores the crucial role of an external LR modulator that modifies receptor–ligand binding affinities, we reasoned that accumulation of Ca^{2+} on one side of the peri-nodal region could locally modulate the activity of the Notch signalling pathway. In this respect, structural analyses of epidermal growth factor (EGF)-like domain-mediated protein–protein interactions suggest that the receptor–ligand affinity and the activity of the Notch signalling pathway are extremely sensitive to Ca^{2+} concentrations[28,29].

We therefore sought to determine whether the extracellular distribution of Ca^{2+} presented any LR bias during chick gastrulation. The use of low-affinity, cell-impermeant Ca^{2+} indicators allowed us to visualize by two-photon excitation microscopy the existence of transient, local accumulations of extracellular Ca^{2+} on the left side of Hensen's node from HH4 to HH6 (Fig. 5a–c). These differences in extracellular Ca^{2+} concentration on either side of the node were no longer evident at HH8 (Fig. 5d). During the revision of this manuscript, evidence for an LR asymmetric distribution of intracellular Ca^{2+} concentrations around the mouse node was reported[30]. The relationship, if any, between this asymmetry in cytoplasmic Ca^{2+} concentrations and the asymmetry reported here warrants further investigation.

To gain further insight into the mechanism responsible for LR differences in extracellular Ca^{2+} concentrations, we cultured HH4–HH6 chick embryos in the presence of omeprazole and analysed the effects of this treatment on Ca^{2+}. A brief (5-min) incubation with omeprazole resulted in the disappearance of the LR difference in Ca^{2+} concentrations (100%, $n = 30$; Fig. 5e–i), showing that the gradient in extracellular Ca^{2+} is a consequence of the differential H^+/K^+-ATPase activity. These results suggest that the alterations induced by omeoprazole on LR determination and on the generation of the Notch activation domain may be related, at least in part, to the suppression of a gradient in extracellular Ca^{2+}.

To explore this hypothesis further, we investigated whether restoring asymmetric Ca^{2+} concentrations on the left side of the embryo could rescue the alterations induced by inhibiting the asymmetric H^+/K^+-ATPase activity. Implantation of beads soaked in omeprazole into HH3–HH4 chick embryos resulted in reversed heart looping in a large proportion of embryos (25%, $n = 130$; Fig. 5j–k). Notably, implantation of Ca^{2+}-saturated agarose plugs on the left peri-nodal region of HH4–HH5 chick embryos completely prevented the LR patterning alterations induced by omeprazole (100%, $n = 14$; Fig. 5l).

Ca^{2+} modulates Notch and determines LR asymmetry

The role of the asymmetric concentrations of extracellular Ca^{2+} on

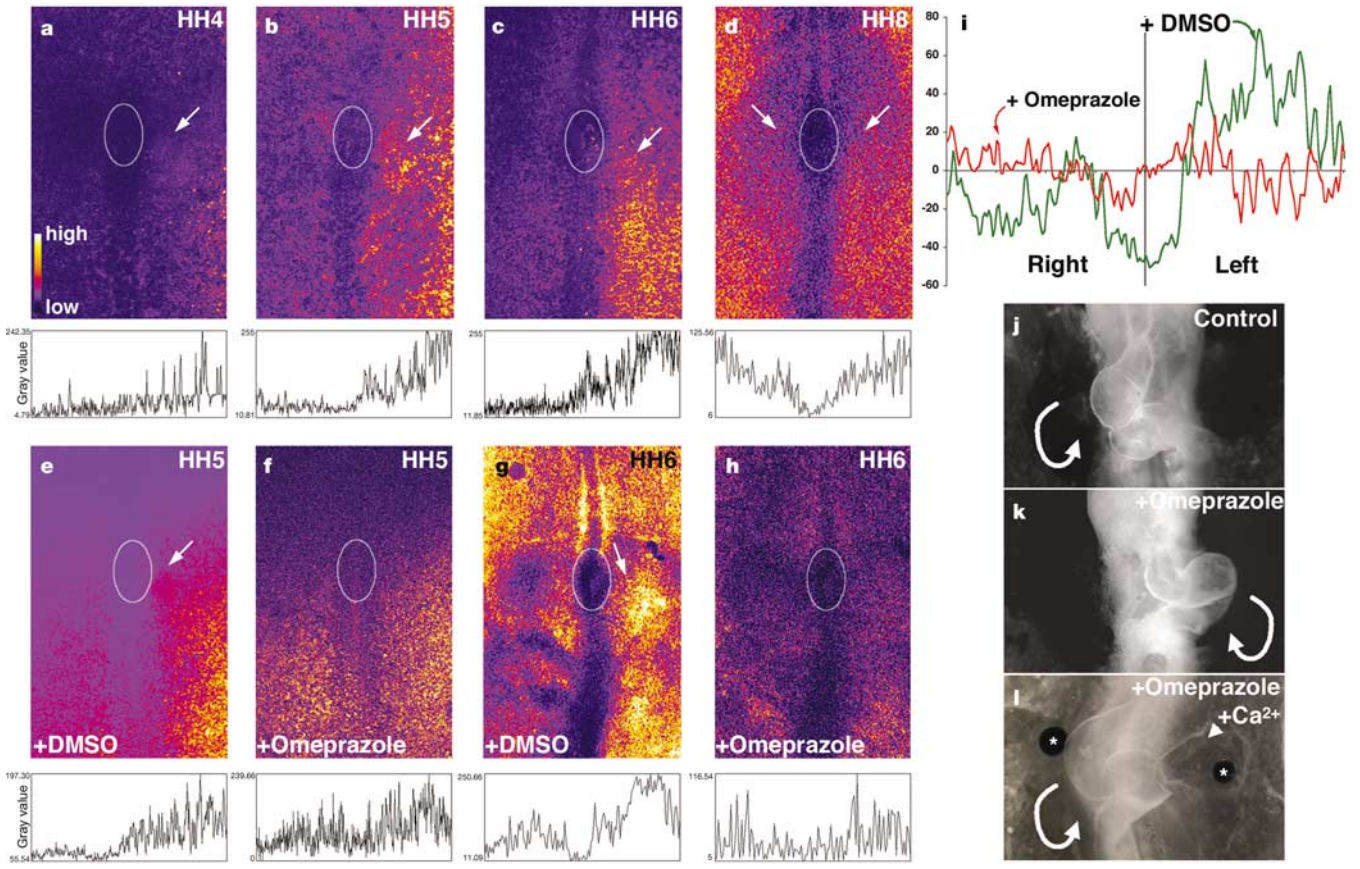

Figure 5 Asymmetric domains of increased Ca^{2+} during LR asymmetry determination. **a**–**d**, Extracellular Ca^{2+} during chick gastrulation was visualized with a cell-impermeant version of the Ca^{2+} indicator Calcium Green-5N. Asymmetric localized domains of increased Ca^{2+} (arrows) appeared on the left side of Hensen's node during HH4–HH6 and became symmetric at HH8. **e**–**h**, Two-photon excitation microscopy images of two representative experiments using chick embryos at HH5 (**e**, **f**) and HH6 (**g**, **h**) show that incubation with omeprazole (**f**, **h**) resulted in disappearance of the asymmetric Ca^{2+} distribution, which was previously visualized in the same embryos treated with the vehicle (DMSO) alone (arrows in **e**, **g**). Embryo views are ventral, anterior is to the top. Ovals mark the position of Hensen's node. In **a**–**h**, grey levels representing fluorescence intensities have been pseudo-coloured with a purple to white scale, and the line scans at the bottom of the images were traced according to Hensen's node coordinates to quantify differences in fluorescence in the same embryos. **i**, Graphs representing the average of normalized fluorescence intensity values for four independent experiments in which Ca^{2+} concentrations were analysed after consecutive incubation with DMSO or omeprazole. **j**–**l**, Alterations in LR organ asymmetries induced by omeprazole (**k**) were prevented by raising Ca^{2+} around the left side of the node (**l**). Semicircular arrows indicate the direction of heart looping. The beads soaked in omeprazole (asterisks) and the Ca^{2+}-saturated agarose plug (arrowhead) are visible in **l**.

LR patterning was directly tested by analysing molecular and morphological landmarks of LR asymmetry after manipulating the extracellular Ca^{2+} concentrations by applying beads coated with the Ca^{2+}-specific chelator BAPTA to HH3 chick embryos. Treatment with BAPTA beads resulted in a high occurrence of the reversal of heart looping (44%, $n = 50$; Fig. 6a, b), an absence of *Nodal* expression around Hensen's node and subsequently in the LPM (35%, $n = 35$; Fig. 6c, d), and a failure to increase activation of Notch signalling around the node, as evaluated by the symmetry of *Dll1* expression at HH5 (33%, $n = 40$; Fig. 6f, g) and of *Lfng* expression at HH6 (40%, $n = 10$; Fig. 6h, i). These results indicate that activation of Notch on the left side of Hensen's node may depend on the local accumulation of extracellular Ca^{2+}. This was further confirmed by expressing active Notch (the intracellular domain of Notch) on the left side of HH3 chick embryos, which rescued the LR defects induced by clamping extracellular Ca^{2+} concentrations with BAPTA (82%, $n = 11$; Fig. 6e).

To investigate whether the mechanism by which extracellular Ca^{2+} regulates Notch activity is direct, we used a co-culture system in which Notch-responding cells are activated by direct contact with cells expressing either Delta1 or Serrate1 ligands[31] and Notch activity is measured by means of a *Hes1*-luciferase reporter[32]. The use of a *Nodal*-based reporter was precluded by the fact that Notch-mediated activation of *Nodal* is restricted to a specific cellular and developmental context (that is, the peri-nodal region of the gastrulating embryo[8,9]), and cannot be mimicked *in vitro* in a co-

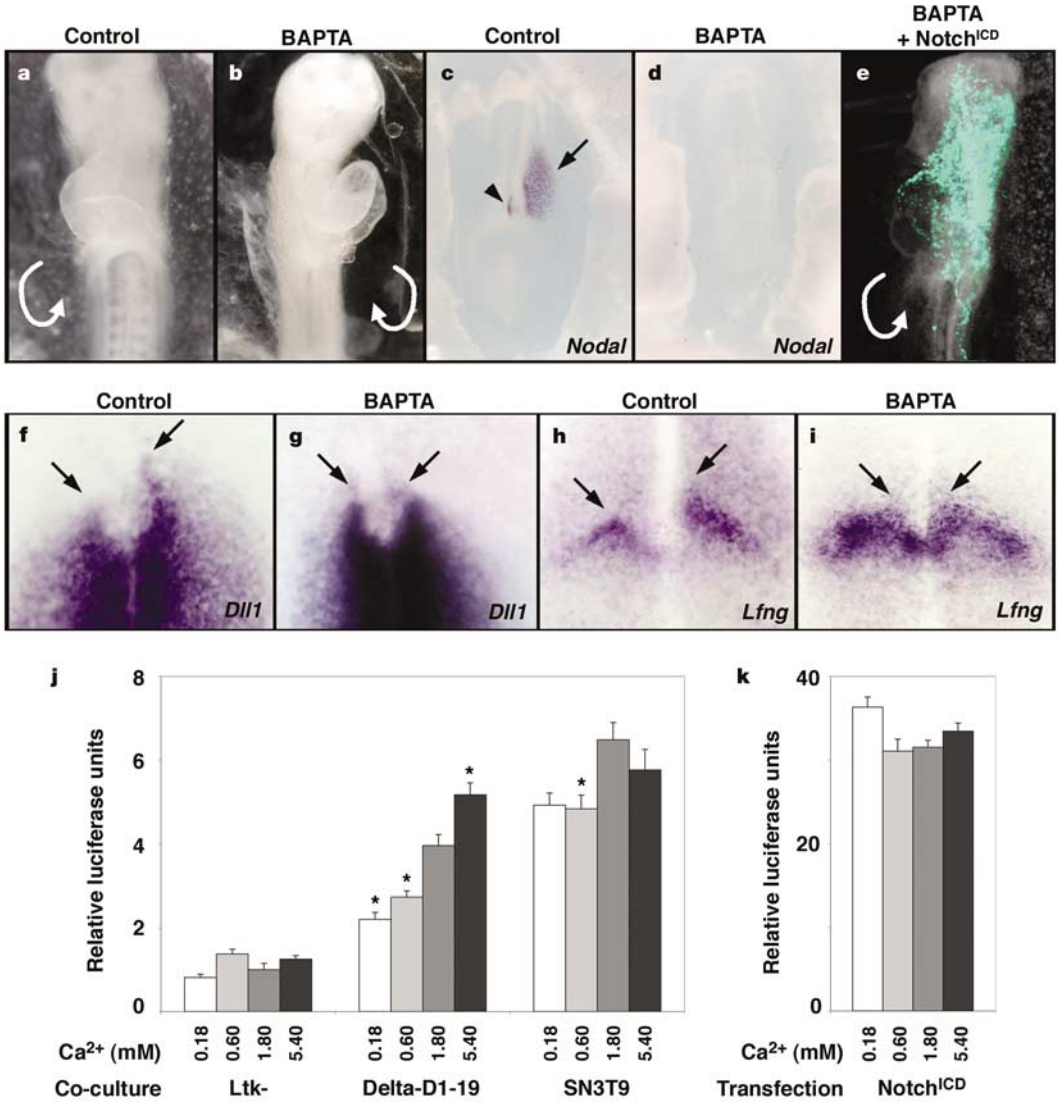

Figure 6 Extracellular Ca^{2+} concentrations directly regulate Notch activity and determine LR asymmetry. **a**–**i**, Clamping extracellular Ca^{2+} concentrations by applying the Ca^{2+}-specific chelator BAPTA coupled to polystyrene beads resulted in alterations in heart looping (**b**), a failure to induce left-sided *Nodal* expression in the node (arrowhead in **c**) and LPM (arrow in **c**), and a loss of the asymmetric expression of *Dll1* (**g**) and *Lfng* (**i**). Arrows in **f**–**i** point to the peri-nodal expression. **e**, Electroporation of an active form of Notch ($Notch^{ICD}$) on the left side of the embryo prevented the alterations in LR organ asymmetry induced by BAPTA. A plasmid expressing EGFP was co-injected to confirm left-side-specific electroporation. Shown is the superposition of dark-field and fluorescence images. Embryo views are ventral, anterior is to the top. Semicircular arrows mark the direction of heart looping. **j**, Notch activity was assayed by co-culturing Notch-responding cells transiently transfected with a *Hes1*–luciferase reporter construct with the mouse fibroblast parental cell line (Ltk-) or with stable lines expressing *Dll1* (Delta-D1-19) or *Jagged1* (SN3T9) in culture medium containing the indicated concentrations of Ca^{2+}. Asterisks indicate statistically significant ($P < 0.05$) differences when compared with Notch activity elicited in medium containing 1.8 mM Ca^{2+} (two-tail Student's *t*-test). **k**, Notch activity induced independently of ligand by the co-transfection of active Notch ($Notch^{ICD}$) did not depend on extracellular Ca^{2+} in the concentration range tested. Luciferase activity was measured after 12 h of co-culture. β-Galactosidase activity was used to normalize for transfection efficiency. Values are expressed relative to the basal Notch activity of Ltk- co-cultures in culture medium containing 1.8 mM Ca^{2+}. Error bars represent the s.d. of three experiments with triplicate measurements.

culture assay (data not shown). By using an approach similar to the one used here, it has been shown that the complete chelation of Ca^{2+} from culture medium results in a ligand-independent induction of Notch activity, owing to dissociation of the non-covalent bond that holds together the intracellular and transmembrane domains of Notch[33]. For this reason, we avoided the use of Ca^{2+} chelators and non-physiologically low concentrations of extracellular Ca^{2+}.

To examine the effect of extracellular Ca^{2+} concentration in Notch activity induced by Delta1 or Serrate1 binding, we used a Ca^{2+}-free medium supplemented with known amounts of $CaCl_2$. Using this system, we were able to detect activation of Notch signalling in a Ca^{2+}- and ligand-dependent manner (Fig. 6j). Notably, we detected statistically significant differences between Notch activities elicited by Delta1 in the presence of Ca^{2+} levels three times lower or higher than the physiological extracellular Ca^{2+} concentration (1.8 mM).

To confirm that the modulation of Notch activity by extracellular Ca^{2+} actually depends on ligand–receptor interactions, we examined the effect of varying Ca^{2+} concentration on the activity of the *Hes1*–luciferase reporter induced by active Notch. We observed potent activation of the Notch reporter that was independent of the Ca^{2+} concentration in the culture medium (Fig. 6k). These results provide strong experimental evidence for a direct mechanism by which extracellular Ca^{2+} concentrations are sensed by the Notch signalling pathway.

Discussion

Our findings represent, to our knowledge, the first evidence that connects extracellular Ca^{2+} signalling with the determination of LR organ asymmetries. Although free cytosolic Ca^{2+} signalling has been described to occur and to be instrumental throughout embryonic development[34], the dynamics of extracellular Ca^{2+} concentrations has been largely overlooked. Our experiments not only identify the existence of localized domains of increased Ca^{2+} concentrations in the gastrulating chick embryo, but also provide direct evidence for a mechanism by which extracellular Ca^{2+} is sensed by the Notch signalling pathway and translated into differential gene expression.

The role of the Notch signalling pathway in providing polarity cues in various organisms, from nematodes to mammals, is well established. Our studies underscore the central role of this pathway during LR determination and identify the existence of a transient, asymmetric domain of Notch activation in the left peri-nodal region. The appearance of this domain depends on a spatio-temporal concurrence of both genetic and epigenetic factors, such that genetic information arranged along the AP axis merges with LR information relayed by Ca^{2+} movements to generate a potent amplification system. The participation of the Notch pathway in LR determination can be understood as a transient and robust mechanism that, acting as a sensor, amplifies local genetic and electro-chemical fluctuations to generate directly a domain of *Nodal* expression. Mechanisms such as the one reported here for organ asymmetry could be operating in other developmental or physiological contexts for the translation of transient epigenetic information into stable patterns of gene expression and, thus, heritable cell fates. □

Methods

Retroviral infection and DNA electroporation

Chick embryos were explanted and grown *in vitro* as described[35]. *RCAS* BP(A) retroviral stocks containing dominant-negative *Su(H)*, dominant-negative *Dll1* or full-length *Lfng* were produced as described[36]. We infected embryos by blastoderm injection at stages HH2–HH4. For electroporation of rat *Delta1* or active *Notch* (both cDNAs were gifts from C. Kintner, Salk Institute, La Jolla, CA), the full-length coding regions were subcloned into a modified pCAGGS vector (Y.K., unpublished data), and a 0.3–0.4 mg ml^{-1} solution of the vector was injected at HH2–HH3. DNA electroporation was done essentially as described[37]. We used five square 50-ms pulses of 10 mV, spaced 350-ms apart. The efficiency and extension of electroporation was monitored by co-injecting 0.05 mg ml^{-1} of pCAGGS–EGFP with the test DNA and examining the fluorescence of enhanced green fluorescent protein (EGFP).

Bead implantation and *in situ* hybridization

BAPTA coupled to polystyrene beads (Calcium Sponge, Molecular Probes) or AffiGel blue beads (BioRad) soaked in DAPT (γ-secretase inhibitor IX, Calbiochem) or omeoprazole (Sigma), or small plugs of 25 mM $CaCl_2$ in 0.5% agarose were applied at stages HH3–HH4 on either side of the chick blastoderm near Hensen's node. Embryos were left to develop and processed for *in situ* hybridization[38] or morphological analysis. Sectioning of stained embryos was done as described[39]. We carried out double-colour *in situ* hybridization essentially as described[40]. Detailed descriptions of the RNA probes and constructs used are available from the authors on request.

Cell culture and reporter assays

The human cervical cancer cell line C-33A (ATCC HTB-31), which expresses *Notch1* (ref. 41) and responds to Notch signalling on the binding of Delta or Serrate ligands (C. Fryers and K. Jones, personal communication), was used as a reporter line in assays of Notch activity. Cells were plated on gelatine-coated 48-well clusters and transfected with different combinations of a *Hes1*–luciferase reporter (ref. 32; a gift from C. Kintner), active Notch and CMX–β-gal plasmids by using standard calcium phosphate transfection protocols (CellPhect, Amersham Biosciences). After 24 h, these cells were co-cultured with either the parental Ltk- mouse fibroblast cell line (ATCC CCL-1.3) or stable derivatives expressing *Delta1* or *Jagged1* (D1-19 (ref. 31) or SN3T9 (ref. 42), respectively; both lines were gifts from C. Fryers and K. Jones, Salk Institute) in culture medium containing different concentrations of $CaCl_2$. Co-cultures were stopped at 2–12 h and assayed for luciferase activity by standard methods. We used β-galactosidase activity to normalize for transfection efficiency. The activity of the reporter is expressed relative to basal values obtained in co-cultures with Ltk- cells in medium containing 1.8 mM $CaCl_2$.

Mathematical modelling

Details of the modelling are given in the Supplementary Methods.

Extracellular Ca^{2+} imaging

Embryos at stages HH3–HH6 were placed in a plastic ring as described[35]. The plastic ring with the embryo was placed in a Wilco dish with a glass bottom and incubated at 38 °C for 15 min with 10 μl of 40 μM Calcium Green-5N, hexapotassium salt (Molecular Probes) diluted in Ca^{2+}-free PBS, pH 7.4. Embryos were imaged on either a 1024 MP (BioRad) or a Radiance 2100 (BioRad) instrument using ×10–20 PlanFluo lenses (Nikon). Two-photon excitation was done at 820 nm with Coherent Mira-Verdi or Tsunami lasers using a pulse width shorter than 150 fs and a 522/DF35 emission filter. Drug-treated embryos were incubated in the presence of 5 μl of 7 μM omeprazole (Sigma), diluted in Ca^{2+}-free PBS from a stock in dimethyl sulphoxide (DMSO; final DMSO concentration $<0.5\%$), and were imaged after omeprazole addition. Before the addition of omeprazole, the embryos were imaged after incubation with equivalent concentrations of DMSO. Images were processed with the ImageJ software (NIH).

Received 11 August; accepted 23 October 2003; doi:10.1038/nature02190.

1. Burdine, R. D. & Schier, A. F. Conserved and divergent mechanisms in left–right axis formation. *Genes Dev.* **14,** 763–776 (2000).
2. Capdevila, J., Vogan, K. J., Tabin, C. J. & Izpisúa Belmonte, J. C. Mechanisms of left–right determination in vertebrates. *Cell* **101,** 9–21 (2000).
3. Mercola, M. & Levin, M. Left–right asymmetry determination in vertebrates. *Annu. Rev. Cell Dev. Biol.* **17,** 779–805 (2001).
4. Hamada, H., Meno, C., Watanabe, D. & Saijoh, Y. Establishment of vertebrate left–right asymmetry. *Nature Rev. Genet.* **3,** 103–113 (2002).
5. Bisgrove, B. W., Morelli, S. H. & Yost, H. J. Genetics of human laterality disorders: insights from vertebrate model systems. *Annu. Rev. Genomics Hum. Genet.* **4,** 1–32 (2003).
6. Brennan, J., Norris, D. P. & Robertson, E. J. Nodal activity in the node governs left–right asymmetry. *Genes Dev.* **16,** 2339–2344 (2002).
7. Saijoh, Y., Oki, S., Ohishi, S. & Hamada, H. Left–right patterning of the mouse lateral plate requires nodal produced in the node. *Dev. Biol.* **256,** 160–172 (2003).
8. Krebs, L. T. *et al.* Notch signaling regulates left–right asymmetry determination by inducing Nodal expression. *Genes Dev.* **17,** 1207–1212 (2003).
9. Raya, A. *et al.* Notch activity induces Nodal expression and mediates the establishment of left–right asymmetry in vertebrate embryos. *Genes Dev.* **17,** 1213–1218 (2003).
10. Artavanis-Tsakonas, S., Rand, M. D. & Lake, R. J. Notch signaling: cell fate control and signal integration in development. *Science* **284,** 770–776 (1999).
11. Hamburger, V. & Hamilton, H. L. A series of normal stages in the development of the chick embryo. *J. Morphol.* **88,** 49–92 (1951).
12. Jouve, C., Iimura, T. & Pourquie, O. Onset of the segmentation clock in the chick embryo: evidence for oscillations in the somite precursors in the primitive streak. *Development* **129,** 1107–1117 (2002).
13. Irvine, K. D. Fringe, Notch, and making developmental boundaries. *Curr. Opin. Genet. Dev.* **9,** 434–441 (1999).
14. Evrard, Y. A., Lun, Y., Aulehla, A., Gan, L. & Johnson, R. L. lunatic fringe is an essential mediator of somite segmentation and patterning. *Nature* **394,** 377–381 (1998).
15. Zhang, N. & Gridley, T. Defects in somite formation in lunatic fringe-deficient mice. *Nature* **394,** 374–377 (1998).
16. Dale, J. K. *et al.* Periodic notch inhibition by lunatic fringe underlies the chick segmentation clock. *Nature* **421,** 275–278 (2003).
17. Geling, A., Steiner, H., Willem, M., Bally-Cuif, L. & Haass, C. A γ-secretase inhibitor blocks Notch signaling *in vivo* and causes a severe neurogenic phenotype in zebrafish. *EMBO Rep.* **3,** 688–694 (2002).

18. Gibson, G. Developmental evolution: getting robust about robustness. *Curr. Biol.* **12,** R347–R349 (2002).
19. Stern, C. D. *et al.* Activin and its receptors during gastrulation and the later phases of mesoderm development in the chick embryo. *Dev. Biol.* **172,** 192–205 (1995).
20. Levin, M., Johnson, R. L., Stern, C. D., Kuehn, M. & Tabin, C. A molecular pathway determining left–right asymmetry in chick embryogenesis. *Cell* **82,** 803–814 (1995).
21. Boettger, T., Wittler, L. & Kessel, M. FGF8 functions in the specification of the right body side of the chick. *Curr. Biol.* **9,** 277–280 (1999).
22. Hirokawa, N. Stirring up development with the heterotrimeric kinesin KIF3. *Traffic* **1,** 29–34 (2000).
23. Wagner, M. K. & Yost, H. J. Left–right development: the roles of nodal cilia. *Curr. Biol.* **10,** R149–R151 (2000).
24. Levin, M., Thorlin, T., Robinson, K., Nogi, T. & Mercola, M. Asymmetries in H^+/K^+-ATPase and cell membrane potentials comprise a very early step in left–right patterning. *Cell* **111,** 77–89 (2002).
25. Stern, C. D. & Wolpert, L. Left–right asymmetry: all hands to the pump. *Curr. Biol.* **12,** R802–R803 (2002).
26. Mercola, M. Left–right asymmetry: nodal points. *J. Cell Sci.* **116,** 3251–3257 (2003).
27. Robinson, K. R. & Messerli, M. A. Left/right, up/down: The role of endogenous electrical fields as directional signals in development, repair and invasion. *Bioessays* **25,** 759–766 (2003).
28. Rao, Z. *et al.* The structure of a Ca^{2+}-binding epidermal growth factor-like domain: its role in protein-protein interactions. *Cell* **82,** 131–141 (1995).
29. Rand, M. D., Lindblom, A., Carlson, J., Villoutreix, B. O. & Stenflo, J. Calcium binding to tandem repeats of EGF-like modules. Expression and characterization of the EGF-like modules of human Notch-1 implicated in receptor–ligand interactions. *Protein Sci.* **6,** 2059–2071 (1997).
30. McGrath, J., Somlo, S., Makova, S., Tian, X. & Brueckner, M. Two populations of node monocilia initiate left–right asymmetry in the mouse. *Cell* **114,** 61–73 (2003).
31. Hicks, C. *et al.* Fringe differentially modulates Jagged1 and Delta1 signalling through Notch1 and Notch2. *Nature Cell Biol.* **2,** 515–520 (2000).
32. Jarriault, S. *et al.* Signalling downstream of activated mammalian Notch. *Nature* **377,** 355–358 (1995).
33. Rand, M. D. *et al.* Calcium depletion dissociates and activates heterodimeric notch receptors. *Mol. Cell. Biol.* **20,** 1825–1835 (2000).
34. Jaffe, L. F. Organization of early development by calcium patterns. *Bioessays* **21,** 657–667 (1999).
35. New, D. A. T. A new technique for the cultivation of the chick embryo *in vitro*. *J. Embryol. Exp. Morphol.* **3,** 326–331 (1955).
36. Ryan, A. K. *et al.* Pitx2 determines left–right asymmetry of internal organs in vertebrates. *Nature* **394,** 545–551 (1998).
37. Itasaki, N., Bel-Vialar, S. & Krumlauf, R. 'Shocking' developments in chick embryology: electroporation and *in ovo* gene expression. *Nature Cell Biol.* **1,** E203–E207 (1999).
38. Izpisúa Belmonte, J. C., De Robertis, E. M., Storey, K. G. & Stern, C. D. The homeobox gene goosecoid and the origin of organizer cells in the early chick blastoderm. *Cell* **74,** 645–659 (1993).
39. Rodríguez-Esteban, C. *et al.* The novel Cer-like protein Caronte mediates the establishment of embryonic left–right asymmetry. *Nature* **401,** 243–251 (1999).
40. Laufer, E., Nelson, C. E., Johnson, R. L., Morgan, B. A. & Tabin, C. Sonic hedgehog and Fgf-4 act through a signaling cascade and feedback loop to integrate growth and patterning of the developing limb bud. *Cell* **79,** 993–1003 (1994).
41. Talora, C., Sgroi, D. C., Crum, C. P. & Dotto, G. P. Specific down-modulation of Notch1 signaling in cervical cancer cells is required for sustained HPV-E6/E7 expression and late steps of malignant transformation. *Genes Dev.* **16,** 2252–2263 (2002).
42. Lindsell, C. E., Shawber, C. J., Boulter, J. & Weinmaster, G. Jagged: a mammalian ligand that activates Notch1. *Cell* **80,** 909–917 (1995).
43. Shi, S. & Stanley, P. Protein O-fucosyltransferase 1 is an essential component of Notch signaling pathways. *Proc. Natl Acad. Sci. USA* **100,** 5234–5239 (2003).
44. Panin, V. M., Papayannopoulos, V., Wilson, R. & Irvine, K. D. Fringe modulates Notch–ligand interactions. *Nature* **387,** 908–912 (1997).
45. Bruckner, K., Perez, L., Clausen, H. & Cohen, S. Glycosyltransferase activity of Fringe modulates Notch-Delta interactions. *Nature* **406,** 411–415 (2000).
46. Moloney, D. J. *et al.* Fringe is a glycosyltransferase that modifies Notch. *Nature* **406,** 369–375 (2000).
47. Murray, J. D. *Mathematical Biology* (Springer, Berlin, 1993).
48. Bosenberg, M. W. & Massague, J. Juxtacrine cell signaling molecules. *Curr. Opin. Cell Biol.* **5,** 832–838 (1993).
49. Collier, J. R., Monk, N. A., Maini, P. K. & Lewis, J. H. Pattern formation by lateral inhibition with feedback: a mathematical model of delta-notch intercellular signalling. *J. Theor. Biol.* **183,** 429–446 (1996).
50. Owen, M. R., Sherratt, J. A. & Wearing, H. J. Lateral induction by juxtacrine signaling is a new mechanism for pattern formation. *Dev. Biol.* **217,** 54–61 (2000).

Supplementary Information accompanies the paper on **www.nature.com/nature**.

Acknowledgements We thank M-F. Schwarz and H. Pineda for their technical skills and dedication; A. Lehrman and H. Juguilon for help with the luciferase assays; G. Sternik for assistance in two-photon excitation microscopy analysis; all laboratory members for discussions; L. Hooks for help in preparing the manuscript; C. Fryers, K. Jones and C. Kintner for reagents and discussions; and T. Gridley and R. Johnson for sharing unpublished results. A.R. is partially supported by a postdoctoral fellowship from the Ministerio de Educación, Cultura y Deporte, Spain; J.R.L is supported by a fellowship from Fundação para a Ciencia e a Tecnologia, Portugal, and M.I. is partially supported by the Fulbright Program and Generalitat of Catalunya. This work was supported by grants from the Fundação Calouste Gulbenkian e Fundação para a Ciencia e a Tecnologia, the American Heart Association, the Human Frontier Science Program, the NIH and the G. Harold and Leila Y. Mathers Charitable Foundation.

Competing interests statement The authors declare that they have no competing financial interests.

Correspondence and requests for materials should be addressed to J.C.I.B. (belmonte@salk.edu).